Effect of oxidized wood flour as functional filler on the mechanical, thermal and flame-retardant properties of polylactide biocomposites

Yunxian Yang[a,b], Laia Haurie[a], Jianheng Wen[c], Shuidong Zhang[c], Arthur Ollivier[b,d], De-Yi Wang[b*]

[a] Department of Tecnologia de l'Arquitectura, Universitat Politècnica de Catalunya, Av. Dr. Marañon 44-50, 08028 Barcelona, Spain

[b] IMDEA Materials Institute, C/Eric Kandel, 2, 28906 Getafe, Madrid, Spain

[c] School of Mechanical and Automotive, South China University of Technology, Guangdong Guangzhou 510640, China.

[d] École Nationale Supérieure de Chimie de Lille, Av. Mendeleïev, 59652 Villeneuve d'Ascq, France.

Corresponding author: deyi.wang@imdea.org

Abstract

Based on the biodegradable material-polyethylene glycol (PEG)-as the plasticizer, oxidized wood flour (OWF) as the charring agent for polylactide (PLA), a series flame-retardant PLA biocomposites were prepared via melt-compounding and hot-compression. The effect of OWF on the thermal, mechanical and flame retardant properties of biocomposites was investigated systemically. We have found that after the incorporation of PEG and OWF with 10wt% into PLA, the biocomposite showed higher tensile elongation than pure PLA. Furthermore, the presence of OWF and ammonium polyphosphate (APP) imparted the biocomposite good flame-retardant performance, shown a remarkable reduction on the peak of heat release rate (PHRR), improved LOI value and passed UL94 V-0 rating. Moreover, Scanning electron microscopy-energy dispersive spectra (SEM/EDS) and thermogravimetric analysis coupled with infrared spectrometer (TG-FTIR) were also performed to understand the flame retardant

mechanism. These results proved that OWF could be as new functional filler for polymer composites to further improve their flame retardancy.

Keywords: Polylactide; Oxidized wood flour; Mechanical properties; Fire behaviors.

1. Introduction

At present, due to more and more serious environment and fire safety problems, environment-friendly flame-retardant composites are studied for its application in many fields, such as transportation, construction, and electrical industries, by more and more researchers. Among various commercial biodegradable polymers, polylactide (PLA) continues occupying a large market due to its renewability, competitive cost, and general mechanical properties. Nevertheless, the intrinsic brittleness and flammability still limit its engineering application (Kuczynski and Boday, 2012; Murariu and Dubois, 2016; Nagarajan *et al.*, 2016). In order to overcome significant drawbacks, several approaches have been conducted, such as chemical modification, blending with plasticizers or fiber reinforcement (Joffre *et al.*, 2017; Lv *et al.*, 2015; Rytlewski *et al.*, 2018; Wang *et al.*, 2014).

One necessary requirement for PLA is to be both tough and strong, yet the two attributes are often mutually exclusive. Furthermore, toughness is a complicated property, which is defined as impact strength or tensile toughness. The former ability is about absorption of impact energy before fracture, while the other is related to yielding strength and multiple crazing during stretched (Nagarajan *et al.*, 2019). An efficient way to enhance the toughness of neat PLA is to blend it with other additives. As a thermoplastic polymer with applications in both construction and furniture industries, polyethylene glycol (PEG) can be used as an efficient toughening agent due to its good plasticity, biocompatibility and biodegradability (Zhang *et al.*, 2013). In

addition, wood flour is also an economical and environment-friendly filler for PLA, and many efforts have already recorded this aspect such as wood plastic composite (WPC) (Orue *et al.*, 2018).

As for the flammability, like conventional polyesters, PLA only illustrates a limiting oxygen index (LOI) value around 20%. The introduction of the flame retardant is a convenient and effective way to get a good flame resistant property. Since halogen-containing flame retardants may produce toxic by-products during the combustion which harm health and environment, in the research field a lot of efforts have been done to develop halogen-free flame retardant systems to polymer (Jian *et al.*, 2018; Schirp and Su, 2016; Shabanian *et al.*, 2013; Yurddaskal and Celik, 2017; Zhang *et al.*, 2018; Zhao *et al.*, 2016). Intumescent flame retardants (IFR) are the most promising alternatives to replace halogen-containing ones and have high flame retardant efficiency (Li *et al.*, 2018a, 2018b). Ammonium polyphosphate (APP) as a halogen-free flame retardant is used in the following study.

In our previous investigations (Zhang *et al.*, 2015, 2009), oxidized starch and regenerated cotton cellulose with higher carboxyl content are proved a higher efficient carbonization agent on IFR for epoxy resin (EP). Wood flour, as an abundant and low-cost renewable natural fibre, is easy to destroy and crash into micro-meter size during oxidization process, which has a similar chemical structure with the two oxidized celluloses above and was already used for improving the thermomechanical properties of epoxy nanocomposites (Saba *et al.*, 2017). Nevertheless, whether the oxidized wood flour (OWF) can act as a higher efficient carbonization agent in flame retardants for PLA or not has been evaluated. Furthermore, many methods only generally affect the mechanical properties, or flame property of PLA separately and a few studies have made efforts to achieve a PLA composite with good mechanical and flame retardant performances simultaneously. In this perspective, this study selected OWF as functional filler to investigate the relationship between fillers' ratio and tensile toughness. After

OWF (as carbonization agent) and APP (as acid source and gas source) were employed to PLA, the flame retardant properties of the biocomposites were also studied.

2. Experimental

2.1 Materials

Polylactide (PLA) 4043D, a multi-purpose extrusion grade, was purchased from NatureWorks (Minnesota, USA). APP was obtained from Budenheim Company (Germany) and PEG6000 was supplied by Sigma-Aldrich. The wood flour (WF) was fabricated by Eulaliopsis binata (EB) with pretreating via continuous screw extrusion steam explosion (Peng *et al.*, 2017). Prior to processing, all the materials were dried at 60 °C under vacuum for 12 h at least.

2.2 Preparation of oxidized wood flour (OWF)

The OWF was prepared by the oxidation of WF, with hydrogen peroxide as the oxidant and $CuSO_4$ as the catalyser (Zhang *et al.*, 2015). The detailed oxidation procedure was: 161 g WF were immersed in 2.5 M NaOH solution for 60 min at 25 °C, then the pH was adjusted to 6.5 by addition of 1.0 mol L^{-1} H_2SO_4 solution. The pretreated WF was rinsed with deionized water to achieve a neutral pH. After that, 2500.0 mL distilled water were added and the temperature increased to 35 °C. 161 mg $CuSO_4$ were dissolved in 500.0 mL of distilled water before being added. The $CuSO_4$ solution was first added to the mixture, followed by the addition of 1 M H_2O_2 in 0.5 h. The mixture was kept at 40 °C with modest stirring for 72 h. The pH value of H_2O_2 was maintained at 6.2 ± 0.2 controlled by 0.1 M $NaHCO_3$ solution. The oxidized fibres were filtered off at the end of the reaction and washed with deionized water. The product was obtained after drying in the vacuum oven at 50 °C for 24 h, and then at 80 °C for 24 h. The carboxyl content of OWF was determined by a method from the United States Pharmacopoeia

(USP, 1995). The OWF with 9.5% carboxyl content was fabricated and used as the filler and carbon source for PLA biocomposites.

2.3 Preparation of PLA biocomposites

For the selection of an optimum ternary system, Table 1A listed a series of biocomposites consisting of PLA/PEG/OWF, which were melt-blended firstly by varying the weight ratios of the three components in a miniature twin screw extruder (MC 15, Xplore) with the rotation rate, mixing temperature and time at 80 rpm, 190 °C and 10 min, respectively. Afterward, all the materials were hot-pressed in a molding machine (LabPro 400, Fontijne Presses), and all the standard test bars for samples were set under a pressure of 2 MPa for 10 min at 190 °C. As for the following tests, the fractions of PLA/PEG/WF were 80/10/10 at weight percentage; meanwhile, the content of APP was fixed at 10 phr on the basis of total composite mass. All the PLA biocomposites were prepared following the procedure described above. All the samples were conditioned for 2 days at 25 °C and 50% RH before mechanical testing. Some relevant information and abbreviations of PLA and its biocomposites are listed in Table 1(b). The binary system of the C4 formulation was only designed as a reference for the thermal and flammability tests.

Table 1 (a). Experimental design of PLA/PEG/OWF

Sample	PLA (wt%)	PEG (wt%)	OWF (wt%)
C-Pre0	80	20	0
C-Pre1	80	15	5
C-Pre2	80	10	10
C-Pre3	80	0	20

Table 1 (b). Experimental design of PLA and its biocomposites

Sample	PLA (wt%)	PEG (wt%)	WF (wt%)	OWF (wt%)	APP* (phr)
C0	100	0	0	0	0
C1	80	10	10	0	0
C2*	80	10	0	10	0
C3	80	10	0	10	10
C4	100	0	0	0	10

APP was fixed at 10phr on the basis of total composite mass.; C2 was equal to C-Pre2.

2.4 characterization

Scanning electron microscopy

Scanning electron microscopy (SEM) and Scanning electron microscopy-energy dispersive spectra (SEM/EDS) were conducted on the equipment (EVO MA15, Zeiss; Helios NanoLab 600i, FEI, German). The PLA biocomposites were cryo-fractured after immersion in liquid nitrogen, and then were coated with a gold layer of 15 nm thickness using a sputter coater (Q150T, Quorum Technologies Ltd., England) before observation at an acceleration voltage of 10KV.

Tensile test

Tensile test was performed on a universal electromechanical testing machine (INSTRON 3384, MA, USA) according to the standard ASTM D638-2014 at room temperature. The crosshead speed was set to 5 mm/min. At least 5 samples were prepared for each composite group and average values were reported.

Thermogravimetric analysis

In order to determine the thermal degradation behavior of PLA and its biocomposites, thermal weight loss curves were obtained from the thermal gravimetric analysis (TGA), which was performed on TGA Q50 instrument (TA Instruments Company). Each specimen with weight of 10 ± 0.5 mg was placed in a platinum crucible and heated from 30 °C to 700 °C at 10 °C/min under a nitrogen flow of 90.0 ml/min.

Limiting oxygen index (LOI)

The flame retardant performance of PLA and its biocomposites (130 mm × 6.5 mm × 3 mm) was characterized by limiting oxygen index (LOI) measurements with a precision of ± 0.2% on oxygen index meter (FTT, UK) according to the ASTM D 2863-2013 standard.

Verticle burning test (UL94)

Standard UL-94 flammability tests (ASTM D 3801-2010) were also performed by UL-94 Horizontal/Vertical Flame Chamber (FTT, UK) on the biocomposite specimens (130 mm × 13 mm × 3 mm) for vertical burning tests.

Cone calorimeter Test (CCT)

Mass loss type cone calorimeter tests (CCT) were carried out by an instrument delivered by Fire Testing Technology Ltd. using the ISO 5660-1 standard method. At least two specimens (100 mm × 100 mm × 3 mm) were exposed to a constant heat flux of 35 kW/m^2 and ignited using a spark igniter. Heat release values and mass reduction were continuously recorded during combustion.

TG-FTIR test

Thermogravimetry-Fourier transforms infrared spectrometry (TG/FTIR) (Q50, TA Instruments Nicolet iS50) was used to study the flame retardant mechanism for PLA biocomposites.

3. Results and Discussion

3.1 Morphological structure

SEM micrographs of the different PLA formulations are shown in Fig. 1. An increase of the OWF up to 10% (C-Pre2) resulted in a more uniform dispersion in the PLA matrix. Figures 1a-d show a smaller particle size, as well as, a good distribution without cracks and holes. However, higher OWF contents, such as 20% (C-Pre3), gave rise to a poor interfacial compatibility.

These results can be probably attributed to the presence of two different phases in the ternary system, PLA/PEG and PEG/OWF, which will not have a good interfacial adhesion until the optimum percentage of each component is reached. Since there was a minimization of the interfacial free energy between phases in a multi-component composite (Guo *et al.*, 1997; Hobbs *et al.*, 1988), it had to destroy two kinds of interfacial energy during tensile fracture. Compared with C2 (PLA/PEG/OWF), the C1 (PLA/PEG/WF) displayed a more defective

morphology with more gaps and large particle agglomerates, which probably lead to a poor interfacial affinity and lower tensile mechanical properties. On the basis of the above results, the brittle-ductile transition would appear at an optimum components' percentage, and the oxidization treatment indeed increased the compatibility between matrices and wood flour.

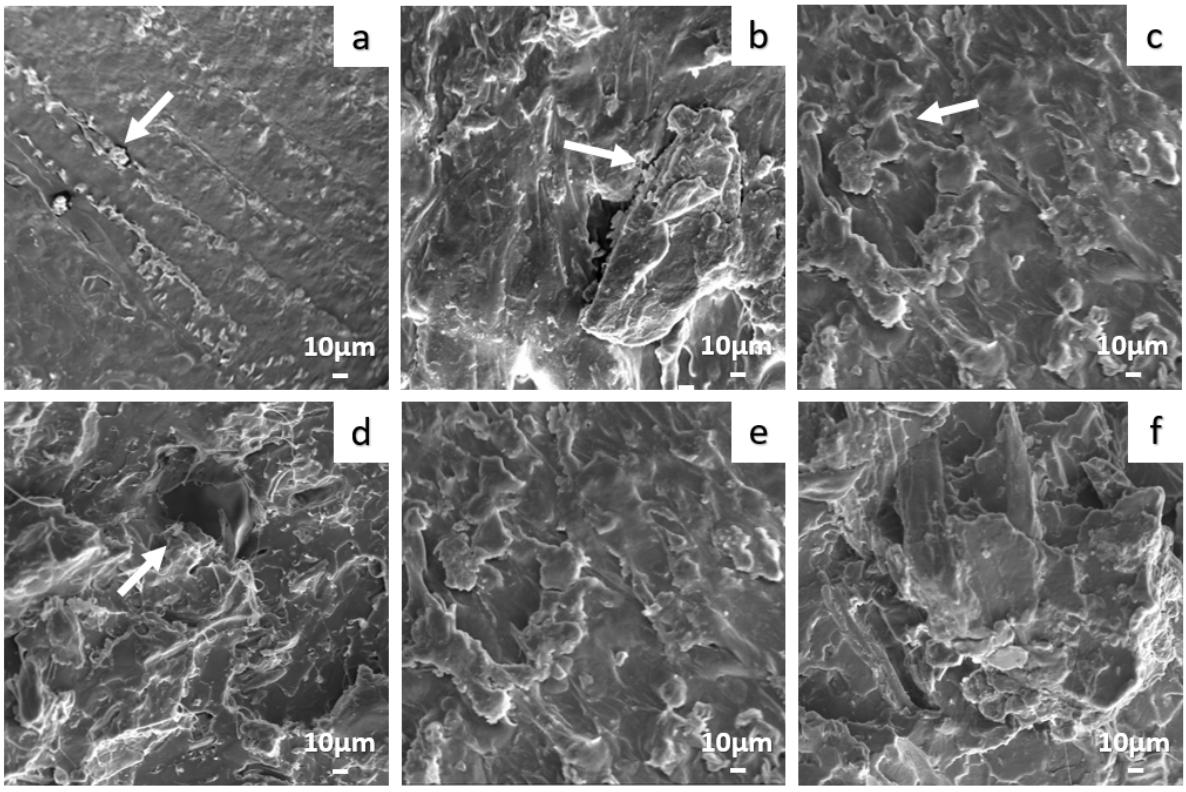

Fig. 1. SEM micrographs of PLA/PEG/OWF biocomposites: a) C-Pre0, b) C-Pre1, c) C-Pre2, d) C-Pre3, e) C2, f) C1

3.2 Mechanical properties

The variation of tensile properties of PLA/PEG/OWF biocomposites was firstly investigated and illustrated in Fig. 2. The blend C-Pre1 with 20 wt% of PEG showed more elongation at break than pure PLA, while exhibited a decrease in tensile strength. This behavior can be explained by the plasticizing effect of PEG on the virgin PLA matrix (Mohapatra *et al.*, 2014). With further increasing OWF incorporation, the composites underwent yielding and stable neck growth through cold drawing during fracture in a tensile test. The optimum value was obtained for the composite C-Pre2 (PLA/PEG/OWF) with 80/10/10 that exhibited more than

68% tensile elongation than neat PLA. This result can be possibly attributed to the reaction between the two additives during processing, which led to a brittle-ductile transition at a proper fraction (Bucknall and Paul, 2009; Dompas and Groeninckx, 1994; Liu *et al.*, 2011). In correspondence to reduced elongation for a binary system composed of PLA and OWF, the increasing content of OWF that improved the stiffness of the system weakened the interfacial regions between matrices and OWF particles, thus made the system more prone to crack propagation and illustrated more brittleness (Afrifah and Matuana, 2013). Therefore, the composite C-Pre2 (PLA/PEG/OWF) with a composition of 80/10/10 had relatively moderate mechanical properties in comparison with neat PLA, which was consistent with the results obtained in SEM.

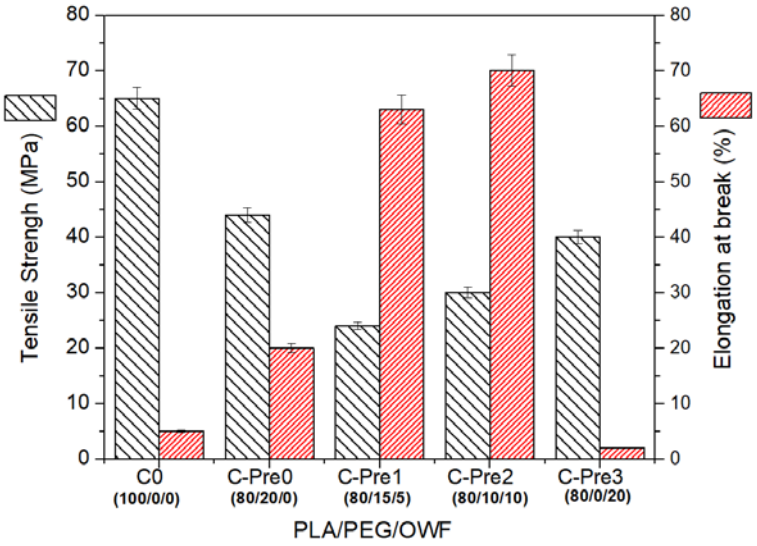

Fig. 2. Tensile stress and elongation of PLA and its biocomposites

Table 2 presented different tensile properties of neat PLA and its biocomposites. Pure PLA demonstrated typical results of a brittle fraction with an elongation at break of ~5.1% and a tensile strength of 67.2 MPa. After adding 10 wt% of PEG and WF respectively, a brittle fraction was also observed for composite C1. The elongation at break was similar to neat PLA, while the stress declined to half with the value of 34.5 MPa. The results were due to the poor interfacial compatibility between components, which lead to more drawbacks and propagated

the cracks during testing. The significant improvement in tensile toughness for C2 with 73.1%, in comparison with C1, suggested that the pretreatment of wood oxidization indeed had a positive effect for compatibility between matrices and wood due to the introduction of the carboxylic group into WF. However, the incorporation of 10 phr APP into the ternary system made the general tensile properties of composite C3 decrease remarkably, and this was because APP interrupted the interaction between phases.

Table 2. Mechanical properties of PLA and its biocomposites

Sample	Tensile strength (MPa)	Tensile modulus (MPa)	Tensile elongation (%)
C0	67.2±0.5	2318±22	5.1±2.0
C1	34.5±1.0	2161±17	4.2±2.0
C2	31.7±1.0	2014±10	73.2±6.0
C3	27.8±1.0	1860±38	9.8±2.0

3.3 Thermal degradation behavior

Thermal stability

TGA was used to evaluate the thermal degradation behavior. The parameters measured included the temperature for 5% mass loss (T_{onset}), maximum degradation and char residue (Cullis and Hirschler, 1983; Hirschler, 1983; Li *et al.*, 2005). The TG curves with a heating rate of 10 °C/min of PLA and its biocomposites were listed in Table 3 and Fig. 3.

From Table 3 and Fig. 3, it can be seen that PLA started to decompose at 326 °C due to the loss of the end group of the main chain or ester change (Li *et al.*, 2009); moreover, there was almost nothing left after 400 °C. The T_{onset} decrease for all the PLA composites. This can be attributed to the poor thermal stability from additives, such as PEG, WF, OWF, and APP, which changed the decomposition temperature of the composites (Song *et al.*, 2011) and also the introduction of carboxyl group would cause a depression in the thermal stability for OWF. However, the residue at high temperature increased after adding the fillers, especially for the composite C3 in which there was the highest residue with 10.3% and 8.9% at 400 °C and

600 °C, respectively. This results from the charring layer formed from the reaction between PEG, OWF, and APP at low temperature to prevent heat reaching the remaining components (Shukor *et al.*, 2014).

Table 3. Results from TGA of PLA and its biocomposites

Sample	T_{onset}*(°C)	Residue (wt%) at	
		400 °C	600 °C
C0	326	0.4	0
C1	313	5.7	2.0
C2	300	5.6	3.0
C3	275	10.3	8.9
C4	317	5.6	5.2

*T_{onset} : the temperature at 5 % mass loss

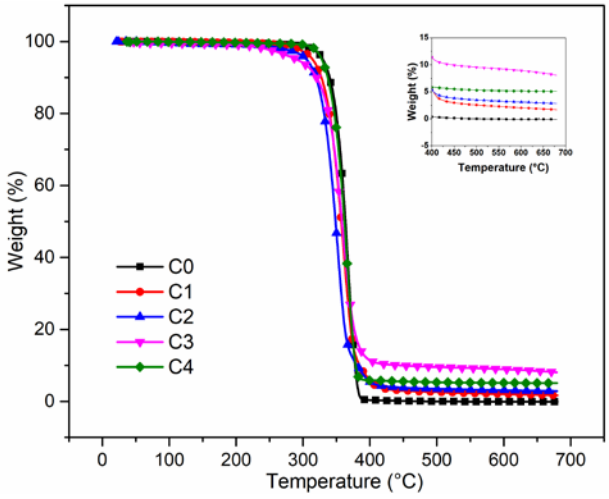

Fig. 3. TG curves of PLA and its biocomposites in nitrogen

Thermal kinetics

Aiming to explain the decomposition behavior of PLA biocomposites (C3 and C4), TG were used to investigate the thermal degradation kinetics in N_2 atmosphere with different heating rates (5, 10, 20, 30, 40 °C/ min). From the Fig. 3, the TG curves of C3 and C4 showed one stage with a char residue of around 10% weight percentage. Nevertheless, some differences in their decomposition behaviors can still be observed from degradation kinetics analysis.

Here, Flynn-Wall-Ozawa method (Ozawa, 1965), which is widely used to determine activation energy directly for given values of conversion, was adopted to analyze the thermal decomposition kinetics of PLA biocomposites. Eq. 1 showed the relationship between activation energy (E_α) and conversion (α)

$$\log \beta = -0.4567 \frac{E_\alpha}{RT} + \left\{ \log \frac{AE_\alpha}{R} - 2.315 - \log F(\alpha) \right\} \quad (1)$$

Where A, E_α, R, β, and T are the pre-exponential factor, degradation activation energy (kJ/ mol), the universal gas constant (8.314 J/ K· mol), heating rate (K/ min) and temperature (K), respectively. And also, g(α) is the integral function of conversion. According to this method, the activation energies E_α for different conversion values can be extracted from the slopes of the lnβ versus 1/T plots (shown in Fig. 4).

From the results listed in Fig. 5, it was noticeable to see that the biocomposite combined with PLA/PEG/OWF/APP exhibited lower degradation energies (E_α) than that only consisted of PLA/APP in the conversion range ($\alpha<0.6$), while the E_α values of the former overtook those of the latter in the further conversion ($\alpha>0.6$). This was because the composite C3 (PLA/PEG/OWF/APP) easily decomposed as compared to C4 (PLA/APP) at the lower temperature ($\alpha<0.6$). However, the charring agents (OWF) interacted with APP to form a stable char layer that hinders the transfer of gas and heat at a higher temperature ($\alpha>0.6$). Therefore, it was necessary to destroy this good physical barrier with high E_α, which was in accordance with the results from TG (Fig. 3).

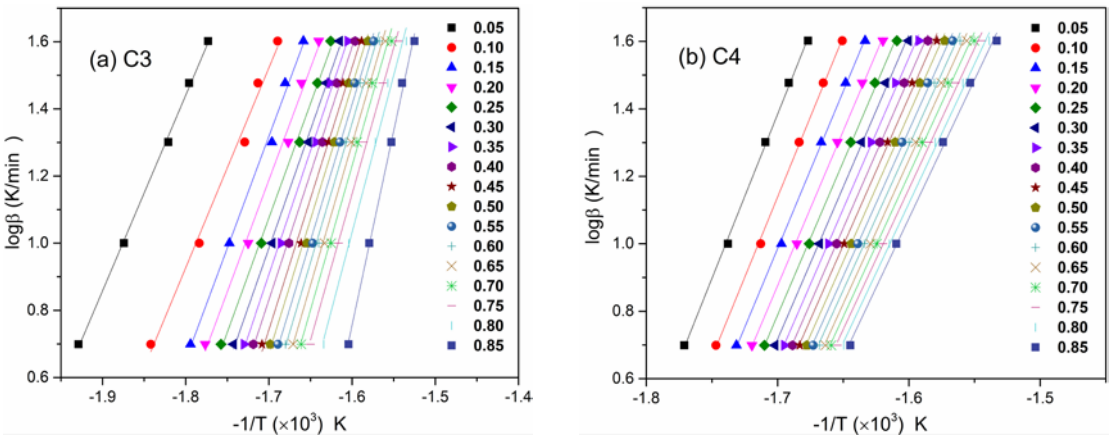

Fig. 4. Plots of logβ against (-1/T) at different heating rates under N_2: a) C3 PLA/PEG/OWF/APP; b) C4 PLA/APP

*Note: The TG curves and correlation coefficient at different heating rates of C3 (PLA/PEG/OWF/APP) and C4 (PLA/APP) were illustrated in supplemental material s-Fig. 1 and s-Table 1.

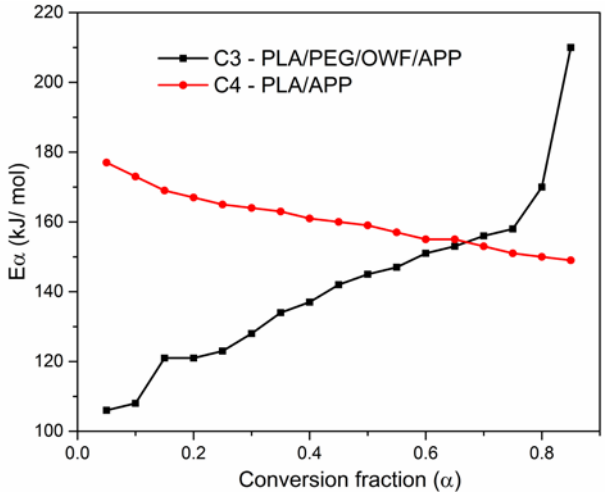

Fig. 5. Activation energies at different conversions obtained by Flynn-Wall-Ozawa method under N_2 atmosphere.

3.4 Burning behavior

LOI and UL-94 test

The LOI and UL-94 of the material are essential indicators of flammability. As for LOI, the material cannot burn until the concentration of oxygen reaches a limiting value; for UL-94,

materials are classified into three rates varied from V-0 to no rating and it is used to determine dripping and flame spreading rates.

The formulation of an intumescent system consists of three components: an acid source, a carbonizing agent and a blowing agent (Laoutid *et al.*, 2009). In this study, while acid parts catalyze the dehydration reaction of the carbonizing agent resulting in the formation of a charring layer, APP played as both acid source and blowing agent and meanwhile wood flour acted as the charring agent in the intumescent flame retardant system due to the existence of hydroxyl groups in its molecular structure (Song *et al.*, 2011).

Table 4 gives the value of LOI and UL-94 for PLA and its biocomposites. It can be seen that all composites except C1 had higher values of LOI than PLA, and the value of LOI for C3 showed 1.3% more than C4, indicating that the incorporation of OWF has more flame retarding effect with APP than only PLA.

The composites (C3 and C4) prepared with APP exhibited UL-94 V-0. This was due to the presence of the APP. Furthermore, the composite C2 reached UL-94 V-2 rate, while the C1 showed no rating, demonstrating that the oxidized modification made wood flour have more char-forming ability than without oxidation.

Table 4. Results of LOI and UL-94 of PLA and its biocomposites

Sample	LOI (%)	UL-94
C0	20.4	No rating
C1	20.0	No rating
C2	21.0	V-2
C3	30.6	V-0
C4	29.3	V-0

Cone calorimeter test

As a useful bench-scale test, the cone calorimeter test (CCT) is a typical technique to simulate the real fire situation in a lab scale, which plays an important role in the quantitative analysis

of the flammability (Lu and Hamerton, 2002; Morgan and Bundy, 2007; Schartel and Hull, 2007). To further investigate the flame resistant property of PLA and its biocomposites, all samples were characterized by CCT. Heat release rate (HRR), peak heat release rate (PHRR), time to ignite (TTI), total heat release (THR) and mass loss (%) were obtained from CCT.

The PHRR is an important parameter to evaluate the intensity of fires (Shi *et al.*, 2009). Fig. 6 summarized the HRR and Table 5 lists the corresponding detail of PHRR date of PLA and its biocomposites. Compared with PHRR of 405 kW/m^2 for neat PLA and that of 403 kW/m^2 for the formulation C4, composite C3 exhibited a lower value of PHRR with 280 kW/m^2, this result reveals the positive synergistic effect from PEG, OWF and APP, which was consistent with the trend from thermogravimetric analysis. However, higher values of 537 kW/m^2 and 522 kW/m^2 were obtained from composites C1 and C2, respectively, this was because the additives of PEG and wood flour lead to a poor thermal stability, but the oxidized pretreatment for wood flour still reduced this value.

The THR values, calculated from the total area under the HRR peaks, is another important parameter used to evaluate fire behavior. There was also a difference in the THR curves for PLA and its biocomposites, shown in Fig. 6. The maximum decrease of THR achieved in composite C3 was 53.5 MJ/ m^2 compared with 68.4 MJ/ m^2 for neat PLA. This was due to the incomplete combustion of the composite undergoing a char-forming process.

Results for TTI and residue, which are also essential indicators of flammability, are displayed in Table 5. Pure PLA started to ignite after 62 s, while its composites showed a lower time to ignition. This was attributed to the addition of fillers with low thermal stability, and the phosphate-containing flame retardants usually decrease the TTI value (Zhang *et al.*, 2014). But meanwhile, the value of residue increased after introduction of wood flour and APP, especially for the composite C3, in which there was 18.4% char residue left while pure PLA almost burned up.

Fig. 7 shows the digital photographs of the PLA and its biocomposites after the cone calorimeter test. It can be noticed that the charring residue for all the samples was different. In neat PLA there was almost nothing left after burning, but the residual char rose after introducing acid source and charring agent. Specifically, the composite C3 greatly swelled with thick and relatively smooth char layer during combustion which exhibited a typical intumescent flame retardant system (Duquesne *et al.*, 2005; Zhu *et al.*, 2011), thus limited the heat and mass exchange between the vapor and solid phases. Compared with C3, the char from composite C4 was thin and loose. All the results above illustrate that OWF has a good synergistic effect with APP and could improve the flame retardant properties of PLA.

Table 5. The results from cone calorimeter test

Sample	PHRR (kW/m²)	TTI (s)	THR (MJ/ m^2)	Residue (wt%)
C0	405±6	62±3	68.4±0.6	0.5
C1	537±5	46±2	64.8±2.0	6.8
C2	522±6	43±1	62.0±1.1	9.0
C3	280±3	40±1	53.5±0.8	18.4
C4	403±3	55±3	56.3±0.8	15.6

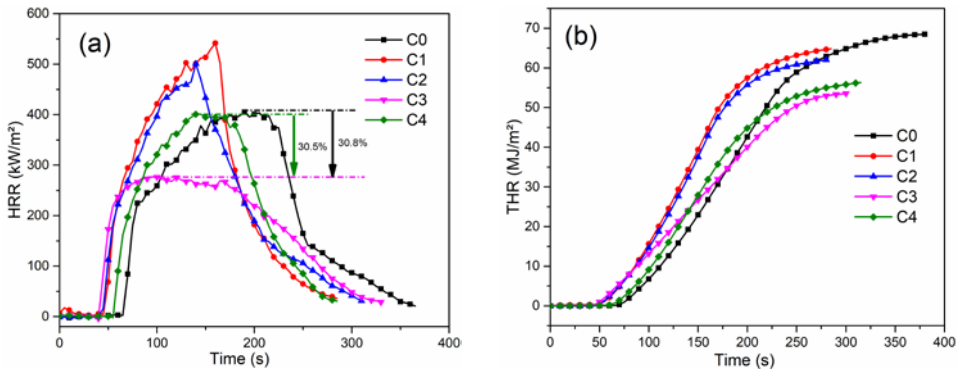

Fig. 6. a) HRR and b) THR curves of PLA and its biocomposites from cone calorimeter test

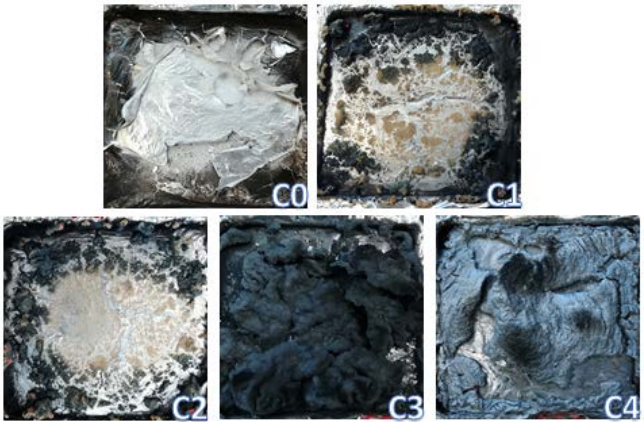

Fig. 7. The digital photographs of the residue after cone calorimeter test: C0 (PLA), C1 (PLA/PEG/WF), C2 (PLA/PEG/OWF), C3 (PLA/PEG/OWF/APP), C4 (PLA/APP)

3.5 Flame retardant mechanism

Due to the presence of APP, the flame retardant mechanism combines phosphorus-nitrogen synergism and intumescent process. As for the condensed phase, scanning electronic microscopy (SEM) and energy dispersive spectra (SEM/EDS) were used to study the char residue of samples after combustion.

With the results from Fig. 8 and Fig. 9, it can be seen that OWF and resin were protected well from the flame in the composite C3, while the composite C4 exhibited a porous and fragile surface. Besides, the SEM/EDS from both internal and external surface illustrated more C and P percentage of the residual char for composite C3 than that for C4. This data offered valuable information to prove that the combination of carbonization agent (OWF) and APP resulted in a char formation on the composite surface. Therefore, the good shield protected PLA and OWF from further decomposition at the higher temperature, eventually improving the flame retardancy. This is consistent with the analysis of the results from CCT.

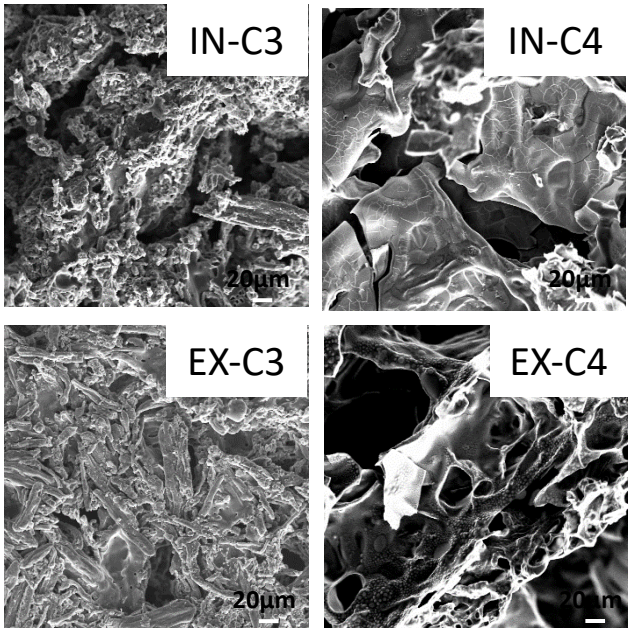

Fig. 8. Morphology of the internal and external charring layer after cone calorimeter test: C3 (PLA/PEG/OWF/APP); C4 (PLA/APP)

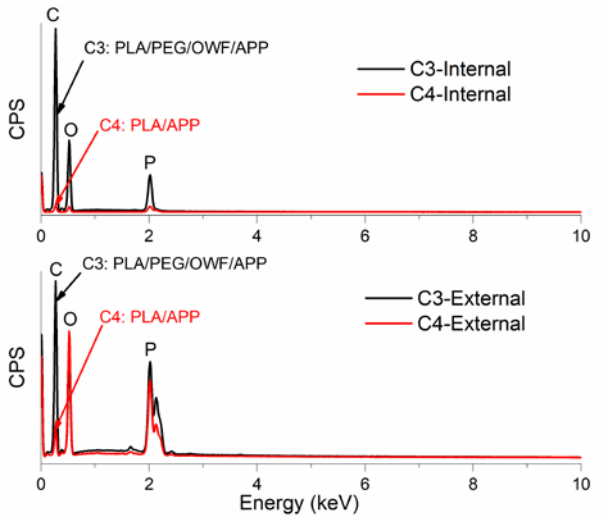

Fig. 9. SEM/EDS of the external and internal charring layer after cone calorimeter test: C3 (PLA/PEG/OWF/APP); C4 (PLA/APP)

To further clarify the flame retardant mechanism, the gas from dehydroxylation, decarboxylation, decarbonylation occurred during combustion process was also analyzed with TG-FTIR.

The major degradable temperature zones of composite C3 (PLA/PEG/OWF/APP) and C4 (PLA/APP) can be extracted from Fig. 3 (from 260 °C to 600 °C), and the FTIR spectra and

the intensity of the evolved gases during combustion were presented in Fig. 10 and Fig. 11. Comparison of FTIR spectra of C3 and C4 demonstrated that the decomposed products presented identical characteristic bands, while the intensity of total evolved gases from C3 was obviously lower than those from C4 during thermal decomposition. Furthermore, compared with C4, the intensity from C-H bond of C3 decreased 33.3%, which was mainly from flammable hydrocarbons (such as backbone of matrix or cellulose). This change proved that acid products from APP acted as charring agent dehydration and charring, and then contributed to form a stable protective layer to retard the transfer of heat, pyrolysis gas products and oxygen (Chen *et al.*, 2010; Ke *et al.*, 2010; Wang *et al.*, 2010), which finally reduced the flammability of C3. Based on the SEM/EDS and TG-FTIR results, the proposed flame retardant mechanism of composite C3 could be interpreted as following (shown in Fig. 12).

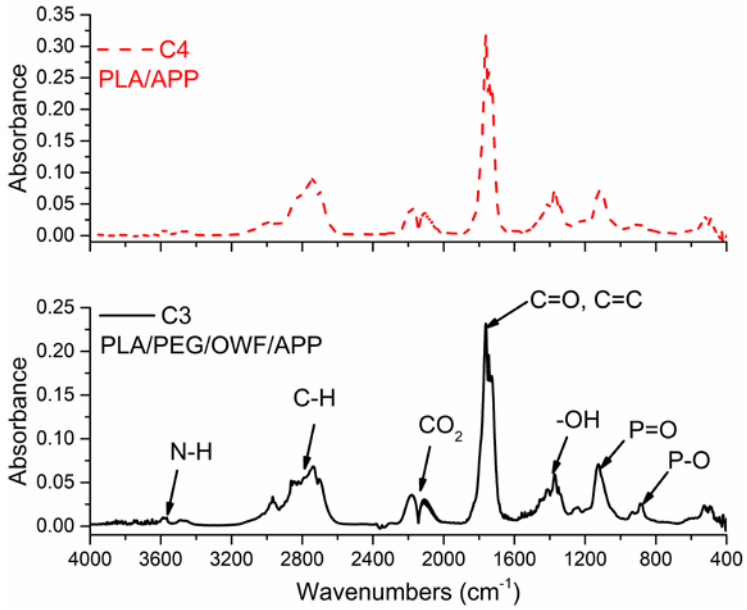

Fig. 10. Spectra of the FTIR from pyrolysis products at T_{max} for C3 and C4.

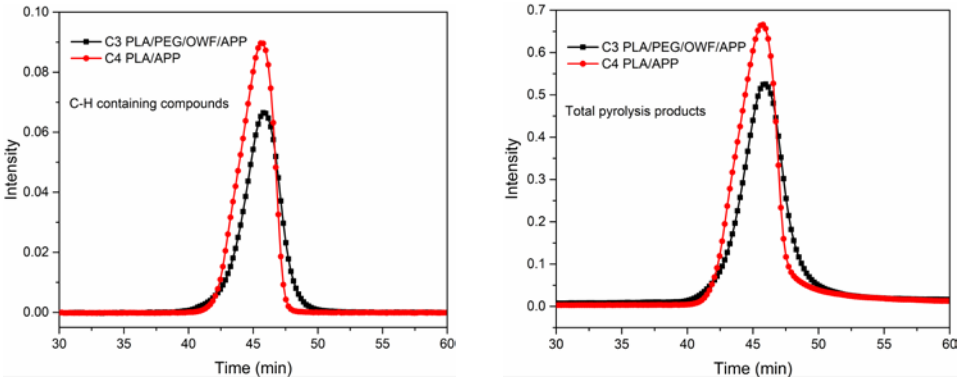

Fig. 11. Relationship between intensity and time of the C-H containing compounds and whole intensity for C3 and C4.

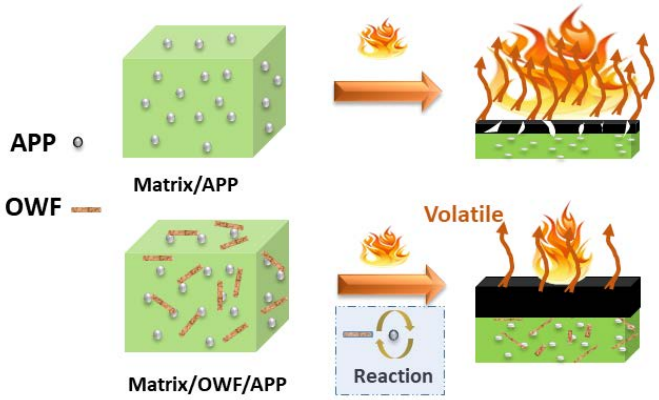

Fig. 12. Proposed flame retardant mechanism for composite C3 and C4.

4. Conclusion

On the basis of the above results and analyses, it is reasonable to state that the PEG and OWF ratio played a critical role in the transition from brittleness to toughness for the ternary composite. When the contents of PEG and OWF were up to 10 wt%, respectively, the elongation at break of the composite C-Pre2 (PLA/PEG/OWF) showed an increase of 68% than that of neat PLA. Moreover, the oxidized pretreatment of wood flour indeed has a positive effect on the compatibility between matrices and wood flour. At the presence of the same contents of wood flour, ternary composite with oxidized wood flour illustrated an increase of 73.1% of tensile toughness than that without oxidization. As for the LOI and UL-94, the same ternary system also reached a 30.6% value and V-0 test. Compared with composite C4

(PLA/APP), the composite C3 (PLA/PEG/OWF/APP) exhibited a more compact char layer with 18.4% residue and less 30.5% of PHRR after combustion, furthermore, high activation energy E_α value resulted to less degraded gas evolved at high temperature (α>0.6). In conclusion, OWF as efficient carbonization agent imparted better flame retardancy to PLA/PEG/APP system.

Acknowledgment

This research is partly funded by Spanish Ministry of Economy and Competitiveness (MINECO) under the projects BIA2014-52688-R, BIA2017-88401-R AEI/FEDER/UE, COMETAD (MAT2014-60435-C2-2-R), Ramón y Cajal fellowship (RYC-2012-10737). It is also partly supported by the Joint Research Fund for Overseas Chinese, Hong Kong and Macao Young Scholars (51628301) and China Scholarship Council (No.201608310142).

References

Afrifah, K.A., Matuana, L.M., 2013. Fracture toughness of poly(lactic acid)/ ethylene acrylate copolymer/wood-flour composite ternary blends. Polym. Int. 62, 1053–1058. https://doi.org/10.1002/pi.4391

Bucknall, C.B., Paul, D.R., 2009. Notched impact behavior of polymer blends: Part 1: New model for particle size dependence. Polymer (Guildf). 50, 5539–5548. https://doi.org/10.1016/j.polymer.2009.09.059

Chen, X., Song, L., Yuan, H., 2010. Flammability and Thermal Degradation of Epoxy Acrylate Modified with Phosphorus-Containing Compounds. J. Appl. Polym. Sci. 115, 3332–3338.

https://doi.org/10.1002/app

Cullis, C.F., Hirschler, M.M., 1983. The significance of thermoanalytical measurements in the assessment of polymer flammability. Polymer (Guildf). 24, 834–840. https://doi.org/10.1016/0032-3861(83)90200-8

Dompas, D., Groeninckx, G., 1994. Toughening behaviour of rubber-modified thermoplastic polymers involving very small rubber particles: 1. A criterion for internal rubber cavitation. Polymer (Guildf). 35, 4743–4749. https://doi.org/10.1016/0032-3861(94)90727-7

Duquesne, S., Magnet, S., Jama, C., Delobel, R., 2005. Thermoplastic resins for thin film intumescent coatings - Towards a better understanding of their effect on intumescence efficiency. Polym. Degrad. Stab. 88, 63–69. https://doi.org/10.1016/j.polymdegradstab.2004.01.026

Guo, H.F., Packirisamy, S., Gvozdic, N. V, Meieri, D.J., 1997. Prediction and manipulation morphologies of multiphase polymer blends : 1. Ternary systems. Polymer (Guildf). 38, 785–794. https://doi.org/10.1016/S0032-3861(96)00571-X

Hirschler, M., 1983. Thermal analysis and flammability of polymers Effect of halogen-metal additive systems. Eur. Polym. J. 19, 121–129.

Hobbs, S.Y., Dekkers, M.E.J., Watkins, V.H., 1988. Effect of interfacial forces on polymer blend morphologies. Polymer (Guildf). 29, 1598–1602. https://doi.org/10.1016/0032-3861(88)90269-8

Jian, R., Xia, L., Ai, Y., Wang, D., 2018. Novel Dihydroxy-Containing Ammonium Phosphate Based Poly (Lactic Acid): Synthesis , Characterization and Flame Retardancy. https://doi.org/10.3390/polym10080871

Joffre, T., Segerholm, K., Persson, C., Bardage, S.L., Luengo, C.L., Isaksson, P., 2017. Characterization of interfacial stress transfer ability in acetylation-treated wood fibre

composites using X-ray microtomography. Ind. Crop. Prod. 95, 43–49. https://doi.org/10.1016/j.indcrop.2016.10.009

Ke, C.H., Li, J., Fang, K.Y., Zhu, Q.L., Zhu, J., Yan, Q., Wang, Y.Z., 2010. Synergistic effect between a novel hyperbranched charring agent and ammonium polyphosphate on the flame retardant and anti-dripping properties of polylactide. Polym. Degrad. Stab. 95, 763–770. https://doi.org/10.1016/j.polymdegradstab.2010.02.011

Kuczynski, J., Boday, D.J., 2012. Bio-based materials for high-end electronics applications. Int. J. Sustain. Dev. World Ecol. 19, 557–563. https://doi.org/10.1080/13504509.2012.721404

Laoutid, F., Bonnaud, L., Alexandre, M., Lopez-Cuesta, J.M., Dubois, P., 2009. New prospects in flame retardant polymer materials: from fundamentals to nanocomposites. Mater. Sci. Eng. R Reports 63, 100–125. https://doi.org/10.1016/j.mser.2008.09.002

Li, Q., Jiang, P., Su, Z., Wei, P., Wang, G., Tang, X., 2005. Synergistic effect of phosphorus, nitrogen, and silicon on flame-retardant properties and char yield in polypropylene. J. Appl. Polym. Sci. 96, 854–860. https://doi.org/10.1002/app.21522

Li, S., Yuan, H., Yu, T., Yuan, W., Ren, J., 2009. Flame-retardancy and anti-dripping effects of intumescent flame retardant incorporating montmorillonite on poly (lactic acid). Polym. Adv. Technol. 20, 1114–1120. https://doi.org/10.1002/pat.1372

Li, Z., Liu, Z., Dufosse, F., Yan, L., Wang, D., 2018a. Interfacial engineering of layered double hydroxide toward epoxy resin with improved fi re safety and mechanical property. Compos. Part B 152, 336–346. https://doi.org/10.1016/j.compositesb.2018.08.094

Li, Z., Zhang, J., Dufosse, F., Wang, D.-Y., 2018b. Ultrafine nickel nanocatalyst-engineering of an organic layered double hydroxide towards a super-efficient fire-safe epoxy resin via interfacial catalysis. J. Mater. Chem. A 6, 8488–8498. https://doi.org/10.1039/C8TA00910D

Liu, H., Song, W., Chen, F., Guo, L., Zhang, J., 2011. Interaction of microstructure and interfacial adhesion on impact performance of polylactide (PLA) ternary blends. Macromolecules 44, 1513–1522. https://doi.org/10.1021/ma1026934

Lu, S.Y., Hamerton, I., 2002. Recent developments in the chemistry of halogen-free flame retardant polymers. Prog. Polym. Sci. 27, 1661–1712. https://doi.org/10.1016/S0079-6700(02)00018-7

Lv, S., Tan, H., Gu, J., Zhang, Y., 2015. Silane modified wood flour blended with poly(lactic acid) and its effects on composite performance. BioResources 10, 5417–5425. https://doi.org/10.15376/biores.10.3.5417-5425

Mohapatra, A.K., Mohanty, S., Nayak, S.K., 2014. Fatigue properties of highly oriented polypropylene tapes and all-polypropylene composites. Polym. Compos. 35, 283–293. https://doi.org/10.1002/pc

Morgan, A.B., Bundy, M., 2007. Cone calorimeter analysis of UL-94 V-rated plastics. Fire Mater. 31, 257–283. https://doi.org/10.1002/fam

Murariu, M., Dubois, P., 2016. PLA composites: From production to properties. Adv. Drug Deliv. Rev. 107, 17–46. https://doi.org/10.1016/j.addr.2016.04.003

Nagarajan, V., Mohanty, A.K., Misra, M., 2019. Perspective on Polylactic Acid (PLA) based Sustainable Materials for Durable Applications: Focus on Toughness and Heat Resistance. https://doi.org/10.1021/acssuschemeng.6b00321

Nagarajan, V., Mohanty, A.K., Misra, M., 2016. Perspective on Polylactic Acid (PLA) based Sustainable Materials for Durable Applications: Focus on Toughness and Heat Resistance. ACS Sustain. Chem. Eng. 4, 2899–2916. https://doi.org/10.1021/acssuschemeng.6b00321

Orue, A., Eceiza, A., Arbelaiz, A., 2018. The e ff ect of sisal fi ber surface treatments , plasticizer addition and annealing process on the crystallization and the thermo-

mechanical properties of poly (lactic acid) composites. Ind. Crop. Prod. 118, 321–333. https://doi.org/10.1016/j.indcrop.2018.03.068

Ozawa, T., 1965. A New Method of Analyzing Thermogravimetric Data. Bull. Chem. Soc. Jpn. 38, 1881–1886. https://doi.org/10.1246/bcsj.38.1881

Peng, H., Zhang, S., Yin, Y., Jiang, S., Mo, W., 2017. Fabrication of c-6 position carboxyl regenerated cotton cellulose by H2O2and its promotion in flame retardency of epoxy resin. Polym. Degrad. Stab. 142, 150–159. https://doi.org/10.1016/j.polymdegradstab.2017.05.026

Rytlewski, P., Stepczy, M., Gohs, U., Malinowski, R., Marian, Ż., 2018. Flax fi bres reinforced polylactide modi fi ed by ionizing radiation. Ind. Crop. Prod. 112, 716–723. https://doi.org/10.1016/j.indcrop.2018.01.004

Saba, N., Jawaid, M., Paridah, M.T., Alothman, O., 2017. Physical , structural and thermomechanical properties of nano oil palm empty fruit bunch fi ller based epoxy nanocomposites. Ind. Crop. Prod. 108, 840–843. https://doi.org/10.1016/j.indcrop.2017.07.048

Schartel, B., Hull, T.R., 2007. Development of fire-retarded materials—Interpretation of cone calorimeter data. Fire Mater. 31, 327–354. https://doi.org/10.1002/fam

Schirp, A., Su, S., 2016. Effectiveness of pre-treated wood particles and halogen-free flame retardants used in wood-plastic composites. Polym. Degrad. Stab. 126, 81–92. https://doi.org/10.1016/j.polymdegradstab.2016.01.016

Shabanian, M., Kang, N., Wang, D., Wagenknecht, U., Heinrich, G., 2013. Synthesis of aromatic e aliphatic polyamide acting as adjuvant in polylactic acid (PLA)/ ammonium polyphosphate (APP) system. Polym. Degrad. Stab. 98, 1036–1042. https://doi.org/10.1016/j.polymdegradstab.2013.02.007

Shi, Y., Kashiwagi, T., Walters, R.N., Gilman, J.W., Lyon, R.E., Sogah, D.Y., 2009. Ethylene

vinyl acetate/layered silicate nanocomposites prepared by a surfactant-free method: Enhanced flame retardant and mechanical properties. Polymer (Guildf). 50, 3478–3487. https://doi.org/10.1016/j.polymer.2009.06.013

Shukor, F., Hassan, A., Saiful Islam, M., Mokhtar, M., Hasan, M., 2014. Effect of ammonium polyphosphate on flame retardancy, thermal stability and mechanical properties of alkali treated kenaf fiber filled PLA biocomposites. Mater. Des. 54, 425–429. https://doi.org/10.1016/j.matdes.2013.07.095

Song, Y.P., Wang, D.Y., Wang, X.L., Lin, L., Wang, Y.Z., 2011. A method for simultaneously improving the flame retardancy and toughness of PLA. Polym. Adv. Technol. 22, 2295–2301. https://doi.org/10.1002/pat.1760

Wang, D.Y., Leuteritz, A., Wang, Y.Z., Wagenknecht, U., Heinrich, G., 2010. Preparation and burning behaviors of flame retarding biodegradable poly(lactic acid) nanocomposite based on zinc aluminum layered double hydroxide. Polym. Degrad. Stab. 95, 2474–2480. https://doi.org/10.1016/j.polymdegradstab.2010.08.007

Wang, Y.N., Weng, Y.X., Wang, L., 2014. Characterization of interfacial compatibility of polylactic acid and bamboo flour (PLA/BF) in biocomposites. Polym. Test. 36, 119–125. https://doi.org/10.1016/j.polymertesting.2014.04.001

Yurddaskal, M., Celik, E., 2017. Effect of halogen-free nanoparticles on the mechanical, structural, thermal and flame retardant properties of polymer matrix composite. Compos. Struct. 183, 381–388. https://doi.org/10.1016/j.compstruct.2017.03.093

Zhang, L., Li, Z., Pan, Y., Pérez, A., Hu, S., Zhang, X., Wang, R., Wang, D., 2018. Polydopamine induced natural fi ber surface functionalization : a way towards fl ame retardancy of fl ax / poly (lactic acid) biocomposites. Compos. Part B 154, 56–63. https://doi.org/10.1016/j.compositesb.2018.07.037

Zhang, S., Liu, F., Peng, H., Peng, X., Jiang, S., Wang, J., 2015. Preparation of Novel c-6

Position Carboxyl Corn Starch by a Green Method and Its Application in Flame Retardance of Epoxy Resin. Ind. Eng. Chem. Res. 54, 11944–11952. https://doi.org/10.1021/acs.iecr.5b03266

Zhang, S.D., Zhang, Y.R., Wang, X.L., Wang, Y.Z., 2009. High carbonyl content oxidized starch prepared by hydrogen peroxide and its thermoplastic application. Starch/Staerke 61, 646–655. https://doi.org/10.1002/star.200900130

Zhang, W., Chen, B., Zhao, H., Yu, P., Fu, D., Wen, J., Peng, X., 2013. Processing and Characterization of Supercritical CO 2 Batch Foamed Poly (lactic acid)/ Poly (ethylene glycol) Scaffold for Tissue Engineering Application 3066–3073. https://doi.org/10.1002/app.39523

Zhang, Z., Yuan, L., Liang, G., Gu, A., Qiang, Z., Yang, C., Chen, X., 2014. Unique hybridized carbon nanotubes and their high performance flame retarding composites with high smoke suppression, good toughness and low curing temperature. J. Mater. Chem. A 2, 4975–4988. https://doi.org/10.1039/C3TA14687A

Zhao, X., Juan, S. De, Reyes, F., Li, Z., Llorca, J., Wang, D., 2016. Effect of N , N 0 -diallyl-phenylphosphoricdiamide on ease of ignition , thermal decomposition behavior and mechanical properties of poly (lactic acid). Polym. Degrad. Stab. 127, 2–10. https://doi.org/10.1016/j.polymdegradstab.2016.01.014

Zhu, H., Zhu, Q., Li, J., Tao, K., Xue, L., Yan, Q., 2011. Synergistic effect between expandable graphite and ammonium polyphosphate on flame retarded polylactide. Polym. Degrad. Stab. 96, 183–189. https://doi.org/10.1016/j.polymdegradstab.2010.11.017